Mon. Not. R. astr. Soc. (1970) **150**, 67–91.

INTERSTELLAR SCINTILLATION AND PULSAR INTENSITY VARIATIONS

B. J. Rickett

(Communicated by the Director of the Nuffield Radio Astronomy Laboratories, Jodrell Bank)

(Received 1970 January 23)

SUMMARY

Observations at Jodrell Bank of the intensity variations from ten pulsars are described. Two regimes are established. A pulse-to-pulse fluctuation is imposed at the source, simultaneously over a wide frequency range. Longer term variations show very fine frequency structure, the width of which varies between sources approximately as the inverse square of the dispersion measure. This slow fading is explained in terms of an interstellar scintillation model. Irregularities in the interstellar electron density with deviations of about 0·1 per cent of the mean density and scale of about 10^{11} cm are deduced.

1. INTRODUCTION

The discovery of pulsars by Dr A. Hewish and his colleagues (**1**) has provided insight into some entirely new aspects of our Galaxy. The nature and origin of pulsars, themselves, are only slowly becoming understood as more radio and optical observations are made. The way, however, in which the emitted radio pulses are modified during propagation is already well understood and has been used to determine several properties of the interstellar medium.

The dependence of pulse arrival time on frequency has been shown to obey a simple plasma dispersion law to a high degree of accuracy (**2**), (**3**), (**4**). The derived quantity, the integrated electron density along the line of sight, has now been measured accurately for most pulsars. This will be referred to as the dispersion measure (in units cm^{-3} pc). The mean interstellar electron density can be directly deduced, if the pulsar distance is known. For CP 0328 and NP 0531 distances of 0·8 kpc and 2·0 kpc (**5**), (**6**), (**7**), (**8**) both correspond to about 0·03 electrons per cm^3. Observations of the angle of linear polarization at two or more frequencies have been interpreted as due to Faraday rotation in the interstellar medium. By combining the deduced rotation measures and dispersion measures several observers (**9**)–(**13**) have estimated the longitudinal component of magnetic field in the pulsar lines of sight.

This paper is chiefly concerned with the identification of a further propagation phenomenon. The variations of pulsar intensities have been extensively studied at Jodrell Bank and a component has been isolated, which is clearly caused by interstellar scintillation. Sections 2–4 of this paper are concerned with the methods of observation and analysis of the pulsar intensity variations; Sections 5–7 present the results. In Sections 8–11 the theory of interstellar scintillation is summarized and compared with the results of the long term pulsar fading. Sections 12–13 review the

deductions concerning the interstellar plasma irregularities and their effect on radio astronomy observations. Finally Section 14 outlines some suggested experiments to elucidate further the interstellar scintillation processes.

2. OBSERVATIONS OF PULSAR INTENSITY VARIATIONS

The variability of pulse intensities has been evident in all pulsar observations since their discovery. The first Cambridge recordings (**1**) at 81·5 MHz revealed erratic variations from CP 1919 over time scales of seconds to months. In early observations at Jodrell Bank (**2**), CP 1919 was observed at 408 MHz to remain comparatively steady over a few minutes, but to show a deep fading over 10–30 min. In an attempt to throw some light on the origins of the fluctuations, extensive observations have now been made using the 250-ft telescope at Jodrell Bank at various frequencies from 151 MHz to 1420 MHz. The intensity variations over time scales of seconds to hours have been studied for about ten pulsars. Some preliminary reports of this work have already been published (**16**), (**17**), (**18**).

Conventional radio receivers were used for the observations. A low-noise amplifier (F.E.T. amplifier at 151 MHz and 240 MHz and parametric amplifiers at higher frequencies) was followed by a mixer, I.F. stages (defining the band-pass) and detector. The detected signals were amplified and displayed on a chart recorder and also fed to an analogue-to-digital converter. The chart recorder had a time response of about 0·25 s, while the time constant, before sampling, was set at 10 ms or 30 ms for these observations. A fast galvanometer with an ultra-violet recording system was also used for a qualitative study of the pulse-to-pulse variations. Some examples of such recordings at two or three frequencies simultaneously are shown in Fig. 1.

For quantitative analysis of the variations, pulse intensities have been recorded in two digital forms. The digitized receiver samples at 10 ms intervals were fed to an on-line computer. These were reduced to give either an intensity for each period or a pulse intensity averaged over one (or more) minutes. We will refer to these as single-pulse data and mean-pulse data, respectively. The pulse intensity is here defined as proportional to the mean level inside a window including the pulse, after subtracting the mean receiver level outside this window. It should be stressed that in both types of data the varying structure within the pulse has been removed by smoothing over the window, which was typically 60 ms long. The repetition period and position of the window were selected manually for each observation. Checks were available on-line to ensure correct phasing of the window within the period.

3. METHODS OF ANALYSIS

Intensities were recorded in the two formats from about ten pulsars at one or more frequencies. For each pulsar-frequency combination, fluctuations were observed on one or more time scales (e.g. pulse-to-pulse and minute-to-minute). In each case the analysis has been directed at establishing quantitative estimates of the time scale and decorrelation frequency width for the differing time scales. Only a part of this comprehensive aim has been achieved, but it is hoped that the results are fairly representative.

The methods of analysis for the two formats have been governed by the quality and duration of the data. Typical pulse energies of 10^{-27} joules metre^{-2} Hz^{-1} were

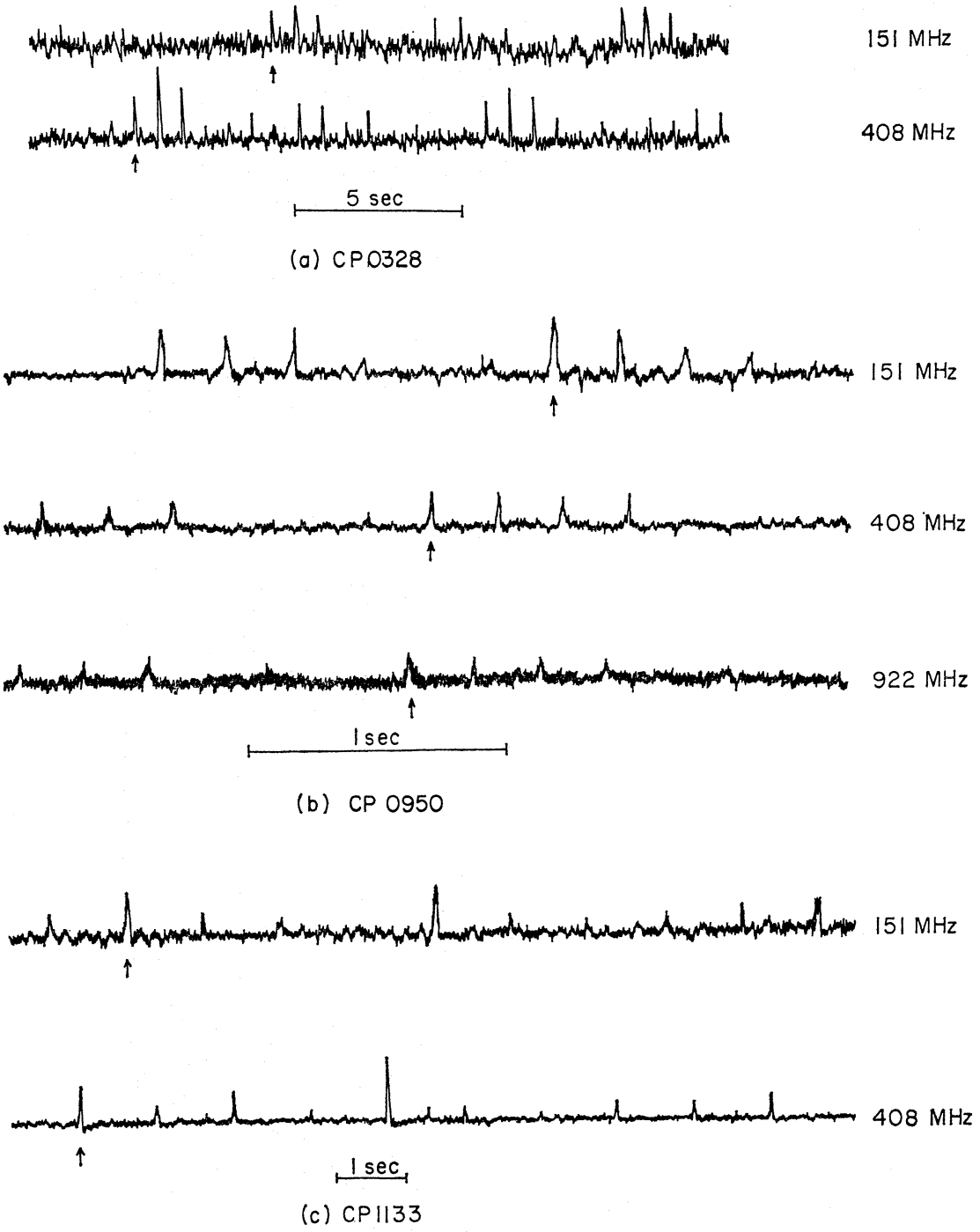

FIG. 1. *Pulse recordings at two or three frequencies with* 30 *ms time constants from* (*a*) *CP* 0328 *in* 4 *MHz bandwidth,* (*b*) *CP* 0950 *in* 1·5 *MHz bandwidth and* (*c*) *CP* 1133 *in* 1·5 *MHz bandwidth. Time increases to the right; the relative dispersion delays are shown by the arrows.*

observed from many of the pulsars, giving an intensity signal roughly equal to r.m.s. noise in a single 60 ms window. Thus for the single-pulse data, satisfactory signal-to-noise ratios were only obtained during the ten-fold increases in signal typical of the slow fading of intensities. In practice, good single-pulse data were obtained for four pulsars. These observations consisted of sequences of several thousand pulses, in some cases at two frequencies simultaneously.

The time scale of the pulse-to-pulse fluctuations has been investigated by forming the auto-correlation function (a.c.f.) out to lags of 64 periods. Slower variations were studied by first smoothing the data into blocks of 5–10 pulses and then forming the a.c.f. Comparison between the frequencies has been made by forming the cross correlation function of the two pulse sequences. An example of the analysis of these observations is shown in Fig. 2. Here, the a.c.f.s and c.c.f. of pulse sequences recorded at 151 MHz and 408 MHz from CP 0328 are shown. Histograms of intensity distributions have also been prepared, an example of which is shown in Fig. 3.

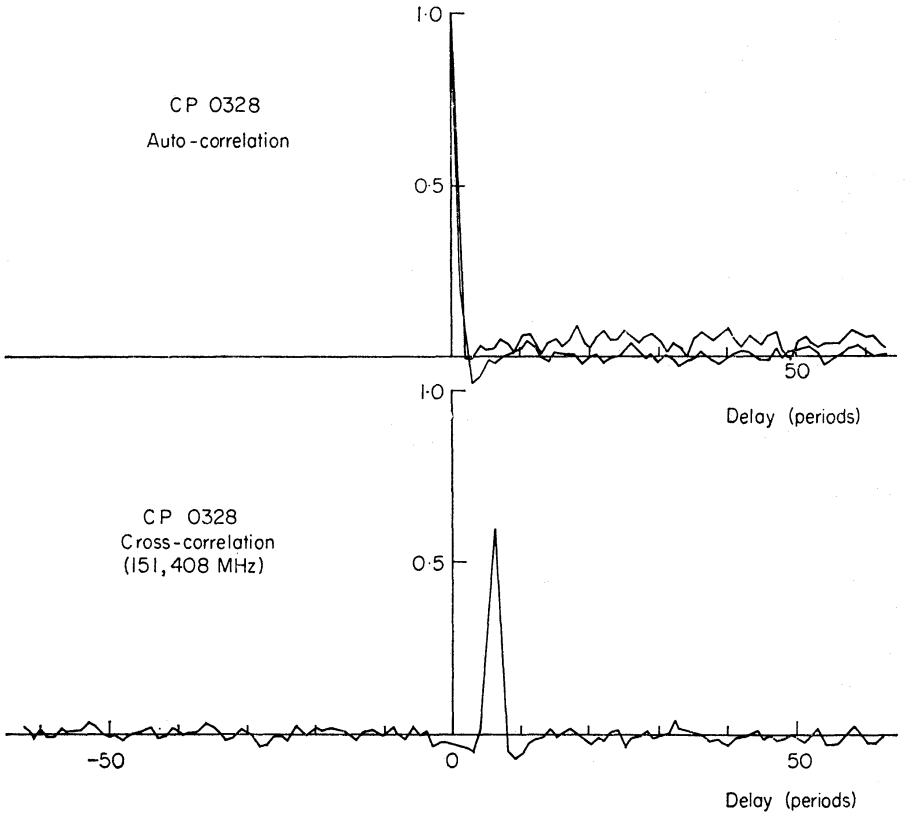

FIG. 2. *Auto and cross-correlation functions of a sequence of* 3500 *pulses from CP* 0328 *at* 408 *MHz and* 151 *MHz in* 1·5 *MHz bandwidths. The dispersion delay of about six periods can be seen.*

For the slower fading, recorded in the mean-pulse format, one minute mean intensities were obtained for runs of one to eight hours from ten pulsars. The noise in these data was down by typically ten times compared with the single-pulse data and satisfactory signal-to-noise ratios were obtained from nearly all the observations. The dominant time scales were in the region 10–100 minutes, giving only a few bursts in the duration of each run. For this reason the auto-correlation analysis was inappropriate and the mean time t_x between maxima in the fading curves has been chosen as a measure of time scale. This quantity is tabulated in Table I for the pulsar frequency combinations observed. The errors (column 3) come from the difficulty in estimating maxima in the presence of noise, and additional errors (column 5) come from the small number of maxima in each observation.

It soon became apparent from mean-pulse recordings made simultaneously at widely-spaced frequencies that the long term fading was completely decorrelated between 151 MHz, 240 MHz, 408 MHz and 922 MHz (see for example Fig. 5 of

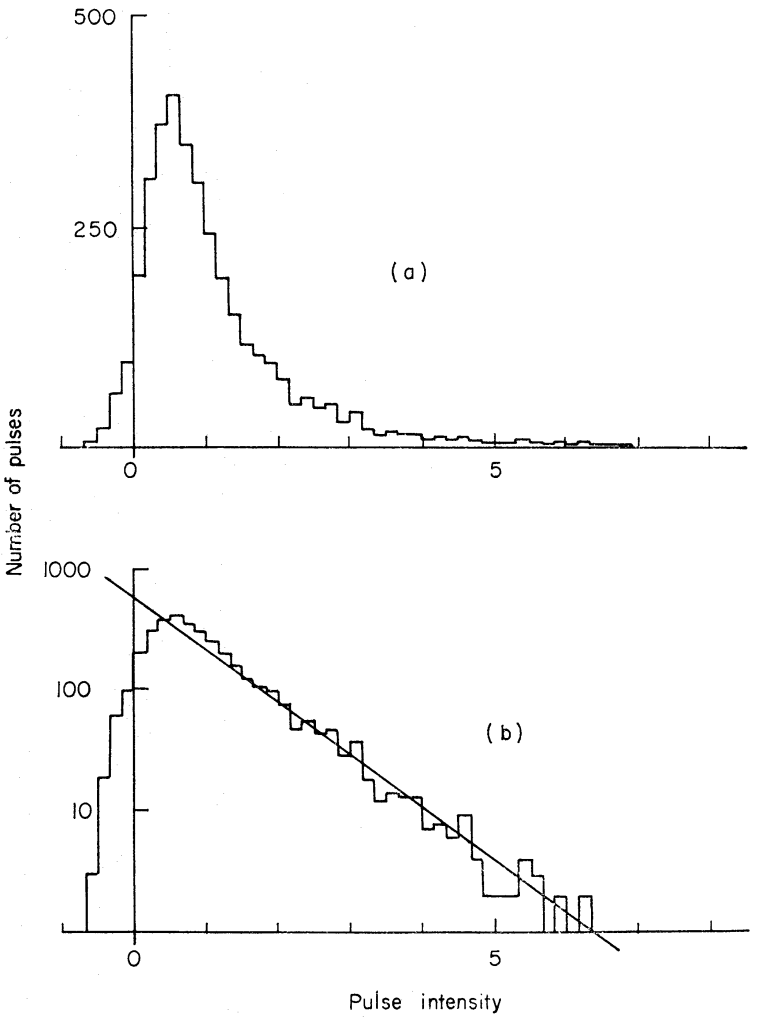

FIG. 3. *Histogram of intensities of a sequence of* 3500 *pulses from CP* 0328 *at* 408 *MHz in* 1·5 *MHz bandwidth. The intensity scale is linear in units of the mean intensity; the number scale is* (*a*) *linear and* (*b*) *logarithmic showing an exponential distribution of the same mean.*

reference (**16**)). A series of observations was thus directed at establishing the frequency width of the long term fading patterns.

Scott & Collins (**19**) were the first to demonstrate the existence of pulsar fine frequency structure in their studies of CP 0950 at 81·5 MHz. For CP 0328 the detailed pulse spectrum at 408 MHz has been studied using the digital spectrometer recently built at Jodrell Bank (**20**). The spectrometer was gated in synchronization with the pulses and spectra were obtained averaged over about seventy pulses. Fig. 4 shows such spectra plotted successively with a resolution of about 60 KHz. The narrow spectral features fade randomly over about four minutes; this is identifiable with a similar time scale observed in the mean-pulse intensity recordings. The fading and the frequency structure are thus clearly part of the same phenomenon.

4. THE BANDWIDTH EXPERIMENT

Investigation with the spectrometer was not possible for the weaker pulsars and a simpler experiment was devised to investigate the frequency structure of as many pulsars as possible. This experiment will be described in some detail as the results are used extensively in later sections.

TABLE I

Time scale of mean pulse data

Source	Frequency (MHz)	t_x (min)	No. of peaks (N)	% Error 100 $(N-1)^{-1/2}$	Averaging time (min)
CP 0328	151	3 ± 1	20	23	1
	408	14 ± 3	20	23	1
	610	18 ± 6	10	31	1
	1420	40 ± 8	80	11	2
CP 0808	151	76 ± 15	5	50	1
	408	170 ± 40	3	70	1
CP 0834	151	12 ± 3	28	19	4
	151	4 ± 2	15	27	1
	408	15 ± 9	30	18	1
	922	21 ± 7	16	26	4
CP 0950	151	78 ± 50	5	50	4
	408	200^{+0}_{-100}	2	100	4
CP 1133	151	11 ± 7	20	23	1, 4
	408	20 ± 10	15	27	1, 4
	922	37 ± 20	9	35	4
HP 1508	151	5 ± 2	20	23	1
	408	7 ± 3	23	21	1
PSR 1749	408	11 ± 5	8	38	1
	610	15 ± 5	5	50	1
CP 1919	151	5 ± 2	40	16	1, 2
	240	7 ± 3	25	21	2
	408	28 ± 8	15	27	2
AP 2015	151	25 ± 15	4	58	1
	408	80 ± 50	2	100	1
PSR 2045	408	8^{+10}_{-2}	11	31	1

Simultaneous observations were made in three bandwidths, typically 0·35 MHz, 1·5 MHz and 4·0 MHz, centred on the same radio frequency. The pulse intensities were plotted versus time as in Fig. 5. Here the fluctuations are more deeply modulated in the narrow than in the wide bandwidths. This can be understood by imagining the spectra of Fig. 4 smoothed with differing bandwidths. The fluctuation index, defined as the r.m.s. deviation normalized by the mean pulse intensity, was determined from the time sequences in each bandwidth. A simple measure of the width of the frequency structure has been defined as that receiver bandwidth which would halve the fluctuation index over that observed in an infinitesimal bandwidth. This is called the half-visibility bandwidth, B_h.

The bandwidth experiment has been performed on nineteen pulsar-frequency combinations and the fluctuation index plotted logarithmically against receiver bandwidth. Fourteen of these plots are displayed in Fig. 6. The index F_b has been corrected for noise, by subtracting the contribution of the noise power to the total fluctuation power, before taking the square root and normalizing. The error bars on

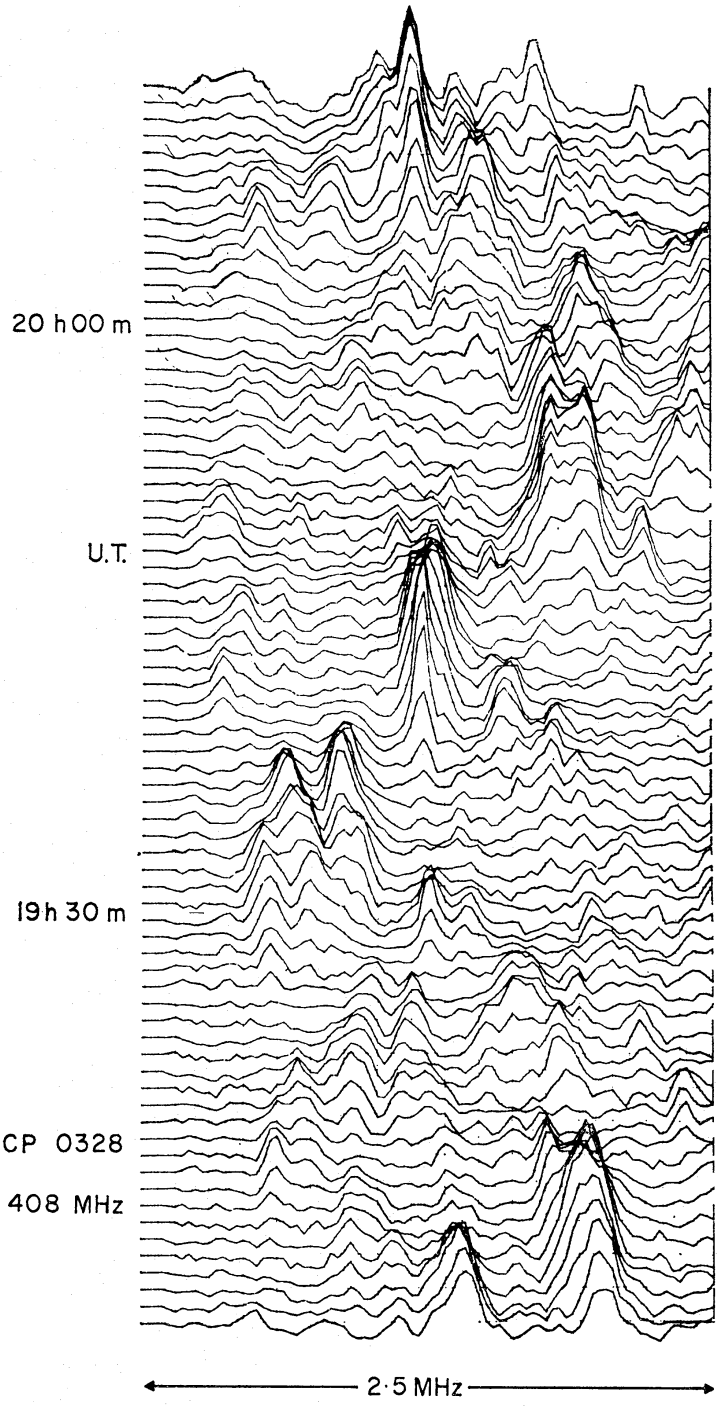

FIG. 4. *Spectra from CP* 0328 *at* 408 *MHz integrated over about* 70 *pulses, plotted at successive* 50 *second intervals. The frequency resolution is about* 60 *KHz and the spectra include the receiver bandpass, which gives a gradual cut-off at the edges of the diagram.*

F_b are due to the uncertainties in the noise correction, and, more important, due to the small number of fading times in the duration of each observation.

The chief difficulty in deducing a value for B_h is that the zero bandwidth index F_0 is not known *a priori*. A simple theoretical model has therefore been fitted to these plots. The model assumes that the fluctuations are statistically stationary and independent with respect to frequency and time. A rectangular bandpass B in width

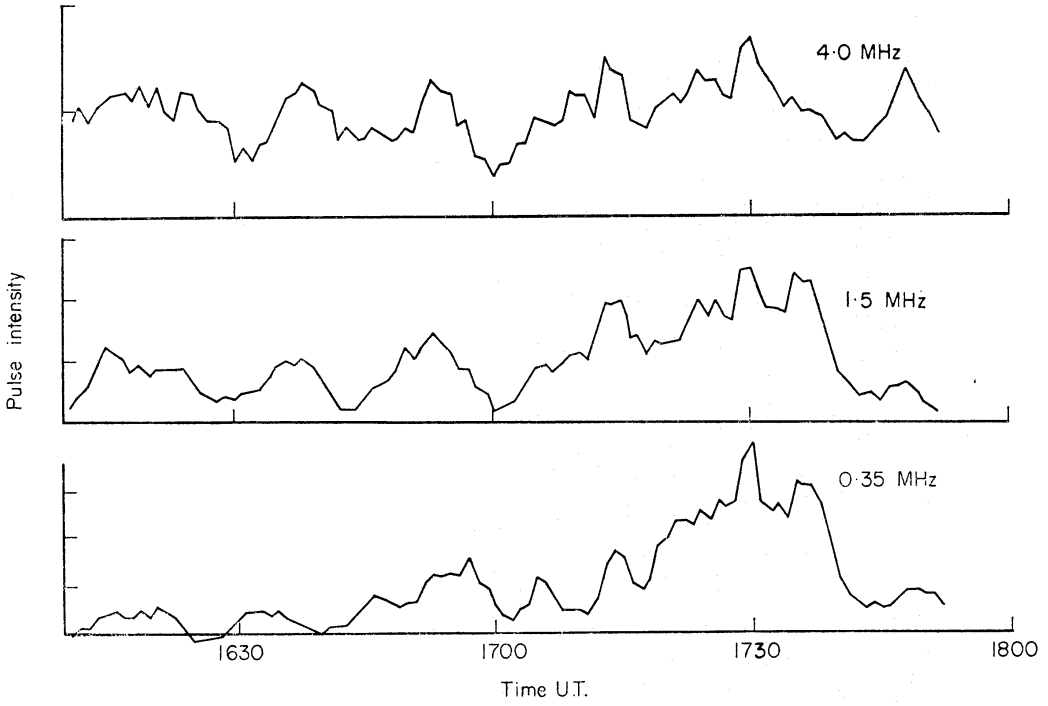

FIG. 5. *The bandwidth experiment on CP 0328 at 408 MHz. Simultaneous recordings of the pulse intensity averaged over 1 minute in the bandwidths indicated.*

is assumed; the normalized a.c.f. for the intensity fluctuations in the frequency domain is assumed to be of the form $\exp(-n^2/n_0^2)$ between frequencies separated by n. It follows that the fluctuation visibility ($V = F_b/F_0$) is given by:

$$V(y) = \{\pi^{1/2}y^{-1}\,\mathrm{erf}\,(y) - y^{-2}(1-\exp(-y^2))\}^{1/2} \qquad (1)$$

where $y = B/n_0$. The model, therefore, gives a single logarithmic curve, equation (1) for F_b against B. Different values of n_0 and F_0 are obtained by shifting the curve horizontally or vertically. The procedure used was to fit a traced version of the curve by eye to the points, taking due account of the error bars. The position of the curve, however, was by no means unique. In the two extreme cases small and large y, a straight line results of slope 0 and $-0{\cdot}5$, respectively. If the points fitted either of these situations only lower or upper limits, respectively, could be deduced for n_0 (and hence for $B_h = 6{\cdot}1\ n_0$).

In arriving at the adopted values of B_h given in Table II a further restriction has been introduced. For the case where the observed points fit a slope of $-0{\cdot}5$, corresponding to bandwidths apparently containing several spectral features, the curve could be moved indefinitely towards smaller values of B_h and larger values of F_0. The value of B_h corresponding to $F_0 = 1$ has then been chosen, with a lower error limit corresponding to $F_0 = 4$. The errors given for B_h are large and somewhat subjective, but it is thought that they do represent the relative confidence to be placed in the results. Table II lists all the results for which a value or limit on B_h could be estimated. Null results were obtained from many 151 MHz observations (e.g. Fig. 6(n)).

Further enquiry has been made into the applicability of the model by analysing the spectra of Fig. 4 in more detail. The two-dimensional a.c.f. with respect to frequency and time has been computed and is shown as a contour diagram in Fig. 7.

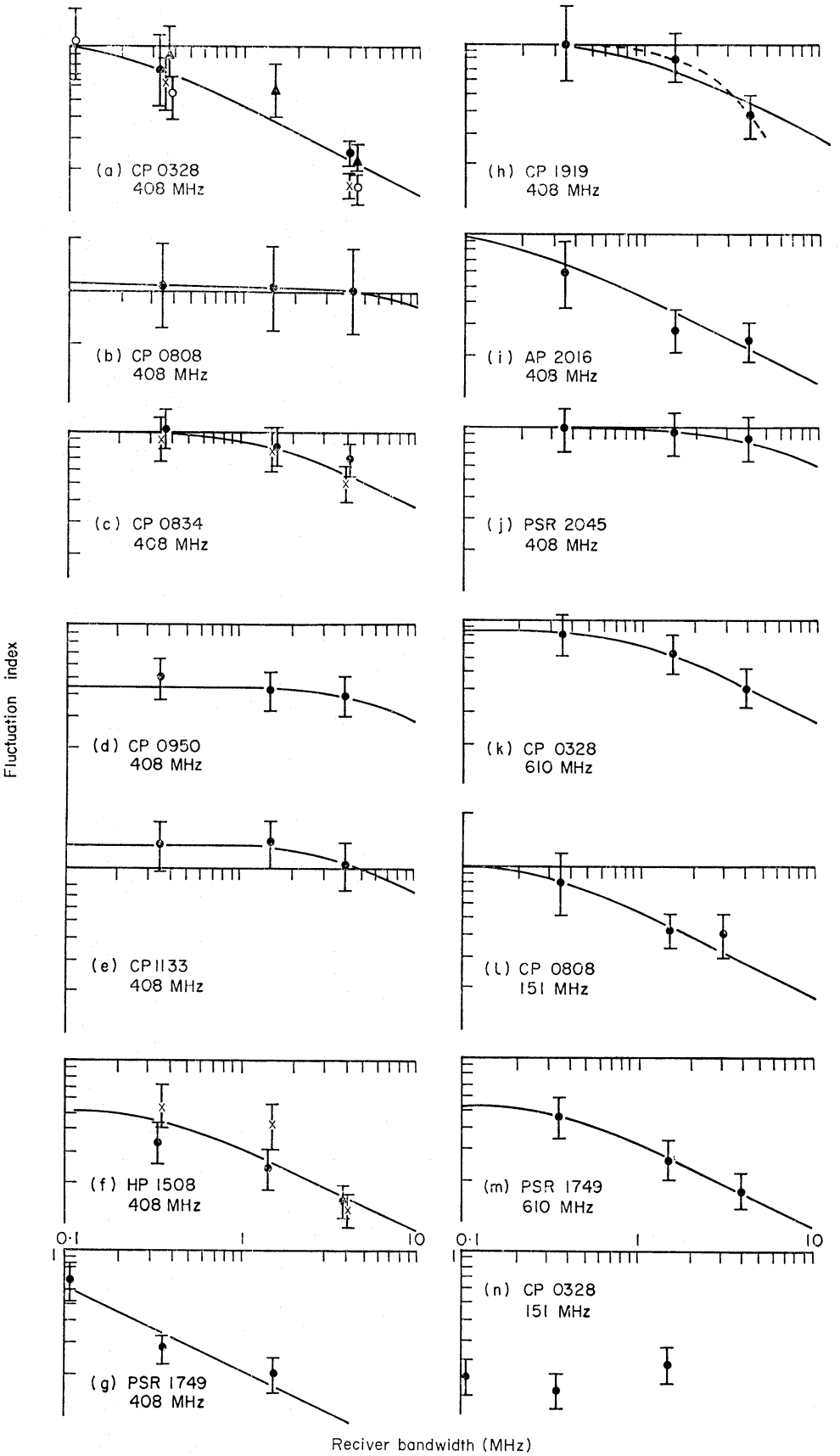

FIG. 6. *Logarithmic plots of fluctuation index versus receiver bandwidth for the pulsar-frequency combinations indicated. The fitted position for the model curve is shown. Different symbols signify observations on separate occasions.*

TABLE II

Half visibility bandwidths

Source	Frequency (MHz)	B_h (MHz)	± dB	F_0	Fig. 6
CP 0328	408	0·8	+ 3 − 6	1·0	(a)
CP 0328	610	4	± 4	0·85	(k)
CP 0808	151	1·2	± 5	1·0	(l)
CP 0808	408	≳ 30		1·1	(b)
CP 0834	408	5·5	± 3	1·0	(c)
CP 0950	408	≳ 20		0·44	(d)
CP 1133	408	≳ 10		1·4	(e)
HP 1508	408	1·5	+ 4 − 6	0·5	(f)
PSR 1749	408	0·15	+ 6 − 10	1·0	(g)
PSR 1749	610	1·5	+ 3 − 5	0·55	(m)
CP 1919	408	3	± 4	1·0	(h)
AP 2015	408	0·7	± 6	1·0	(i)
PSR 2045	408	≳ 18		1·0	(j)

The a.c.f.s. given by cuts along the frequency and time axes are also shown. In the frequency domain the a.c.f. is nearer to exponential than the gaussian (assumed in the model), but this will not significantly affect the values of B_h compared with the uncertainties. The value of B_h computed from the CP 0328 spectra agrees well with that determined from the bandwidth experiment.

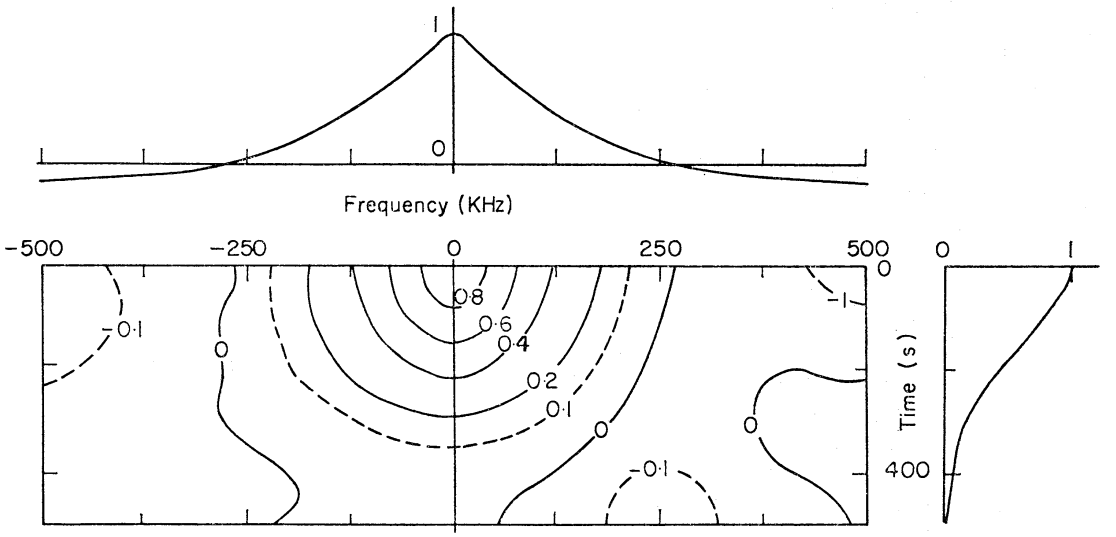

FIG. 7. *Contour diagram of the two dimensional auto-correlation function (in time and frequency) of the data of Fig. 4. Sections along the time and frequency axes are shown.*

5. THE OBSERVED CHARACTERISTICS OF PULSAR INTENSITY VARIATIONS

A summary of the results is now given by, first, considering the fluctuations from CP 0328 over several time scales and at various frequencies and, second, by making comparisons between the pulsars.

The auto-correlation analysis of Fig. 2 has revealed the presence of a deeply modulated pulse-to-pulse variation from CP 0328. This is highly correlated

($\gtrsim$60 per cent) between 151 MHz and 408 MHz. The position of the peak in the c.c.f. at six periods delay corresponds to the dispersion between the two frequencies, We conclude that bursts of 2–3 pulses occur simultaneously at both frequencies. and that this variation is imposed before the pulses travel through the dispersing medium. The negative-going portions of the correlation functions seem to imply that the bursts are followed by relatively inactive periods, with the source only recovering after about ten periods. Dr R. R. Clark (private communication) has observed drifting of the features within the pulse during these bursts. One explanation is that each burst is from a single emitting region (e.g. group of electrons), which may be moving with respect to the star, but which only survives for a few periods of revolution.

In Fig. 1(a) the broad-band nature of the pulse-to-pulse variations is also evident, showing that the ratio of pulse intensities (after removing the dispersion delay) between 151 MHz and 408 MHz remains constant for tens of seconds. However after a few minutes the ratio may have changed substantially; this slow fading constitutes the second regime of the fluctuations. In contrast to the short term variations the long term fading shows very narrow frequency structure (Fig. 4). The intensity varies randomly in frequency and time with $1/e$ decorrelation widths of about 125 KHz and 3·8 minutes, at 408 MHz. Similar data taken at 610 MHz, using six analogue filters covering a total of 2 MHz, gave widths of about 400 KHz and 6 minutes.

We now consider the results from the other pulsars. The long term fading component shows itself in the recordings made in the bandwidth experiment and will be discussed in Section 7. Short term fluctuations, very similar to those observed for CP 0328, have been identified for CP 0950, CP 1133 and PSR 1749-28. For some sources (i.e. CP 1919, CP 0834 and CP 0808) there is much less pulse-to-pulse variation at 408 MHz. For HP 1506, AP 2015 and PSR 2045-16 the data were of inadequate signal-to-noise ratio. The results for CP 1919 are described in the next section. Broad-band short term fluctuations have been reported from NP 0525 and NP 0531 (**21**), (**22**).

6. INTENSITY VARIATIONS FROM CP 1919

As the variations in pulse intensity from CP 1919 cannot immediately be classified into the two regimes mentioned above, some further discussion of its behaviour is necessary. This pulsar is especially interesting as it has been studied extensively by many observers.

At 80–200 MHz it is characterized by bursts of activity lasting about one minute at intervals of several minutes (**1**), (**3**), (**23**), (**24**). At the lower frequencies there is some evidence of pulse-to-pulse variations within the one minute outbursts, though there may be a contribution to this from interplanetary scintillation. At 408 MHz and above the variations are much slower (**2**), (**25**) showing time scales of 10–30 minutes but less pulse-to-pulse variation. Fine frequency structure has been observed in the spectrum at 150 MHz (**24**) and at 430 MHz (**25**). Spaced receiver observations (**26**), (**27**) have shown that the fluctuations, of duration one minute or faster at 80 MHz and 110 MHz, are not caused by interstellar scintillation.

The present observations have included many recordings from CP 1919. Three components appear to be present in the variations. The fastest of these shows a repetition time of 4–5 pulse periods. This was first noted by Conklin *et al.* (**27**) and

explained by Drake & Craft (**28**) as being caused by the pulse drifting phenomenon (known as the second periodicity). The a.c.f.s. at 148 MHz and 151 MHz (Fig. 8) show the effect as small subsidiary peaks. The spikes at zero lag may be due to noise or to a genuine weakly modulated pulse-to-pulse variation.

The second component is characterized by one minute bursts evident at 148, 151, 240 and 408 MHz; these occur as features in the a.c.f.s (Fig. 8) with half-power half widths of about twenty periods, though the depth of modulation is clearly reduced at 408 MHz. The c.c.f.s (Fig. 8) show that these same features are strongly correlated between 148 and 151 MHz and somewhat more weakly correlated between 240 MHz and 408 MHz. The one minute bursts are revealed more clearly by smoothing the pulses into groups of five or ten before computing the a.c.f.s and c.c.f.s. Examples of this are also shown in Fig. 8; these show a tendency for the bursts to repeat at intervals of about 120 pulses. A period of 120 pulses corresponds to $6{\cdot}3 \times 10^{-3}$ Hz; the power spectrum of Lovelace & Craft (**25**) at 112 MHz shows a significant peak at 6×10^{-3} Hz, supporting the identification of a quasi-periodic variation.

The third component of the variations from CP 1919 is identifiable with the long term fading of other sources. At 408 MHz it is the dominant component and is responsible for the fading over times of 10–30 minutes, and associated frequency structure of a few MHz in width. At 151 MHz the fading time is faster and frequency width narrower. Komesaroff *et al.* (**24**) observed decorrelation over 0·5 MHz over a few minutes at this frequency. The present observations at 148 and 151 MHz showed a ratio of pulse intensities, which was constant over 1–2 minutes but changed over 5–10 minutes.

The interpretation of these results for CP 1919 is that the first rapid component is intrinsic to the source and is associated with the ' second periodicity '. The third fading component is identified with the long term regime of other pulsars. The second component has no direct counterpart, but is a broad-band variation like the short term regime of other pulsars. It is slower (minutes compared to seconds) and the depth of modulation decreases with increasing frequency. It seems possible that this component is due to a scintillation caused in a ' screen ' close to the source, which becomes ' phase thick ' at about 200 MHz. However, the quasi-periodic nature of the variations is not readily explained on this hypothesis. Bearing these considerations in mind it seems best at this stage to classify the second component under the short term regime.

Other sources, possibly showing a similar shallow variation at 408 MHz over a time scale of minutes, are CP 0834 and CP 0808.

7. THE LONG TERM FADING

The fading component of pulse intensities is characterized by variations over a time scale of minutes to hours, with which is associated narrow frequency structure from 100 KHz to 10 MHz in width. We first summarize the results for ten pulsars at 408 MHz, and then compare the behaviour at different frequencies for a few pulsars. The results in question are depth of fluctuation, time scale and frequency width.

The chief source of data is the bandwidth experiment, in which the fluctuation index F_0 for zero bandwidth was determined only very approximately. The conclusion is that indices F_0 normally lie in the range 0·5 to 1·3; values larger than one

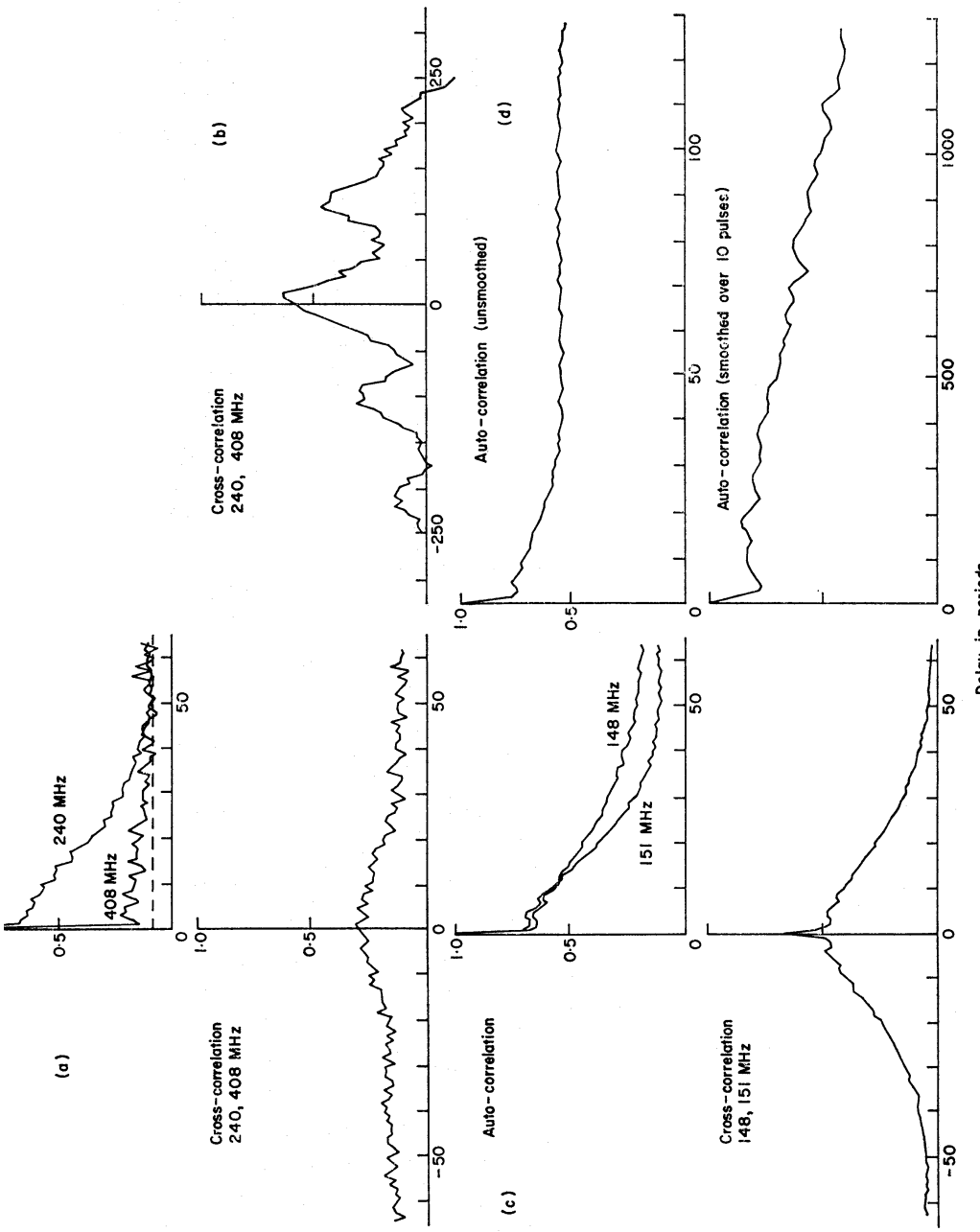

FIG. 8. *Auto-correlation and cross-correlation functions (a.c.f. and c.c.f.) of pulse sequences recorded from CP 1919. The frequencies and bandwidths are indicated. (a) 2 MHz bandwidth at 240 MHz and 4 MHz at 408 MHz, 830 pulses unsmoothed. (b) As (a) but first smoothed over 5 pulses. (c) 1 MHz bandwidths at 148 MHz and 151 MHz, 3000 pulses unsmoothed. (d) 4 MHz bandwidth at 408 MHz, 7200 pulses unsmoothed (upper curve), and smoothed over 10 pulses (lower curve).*

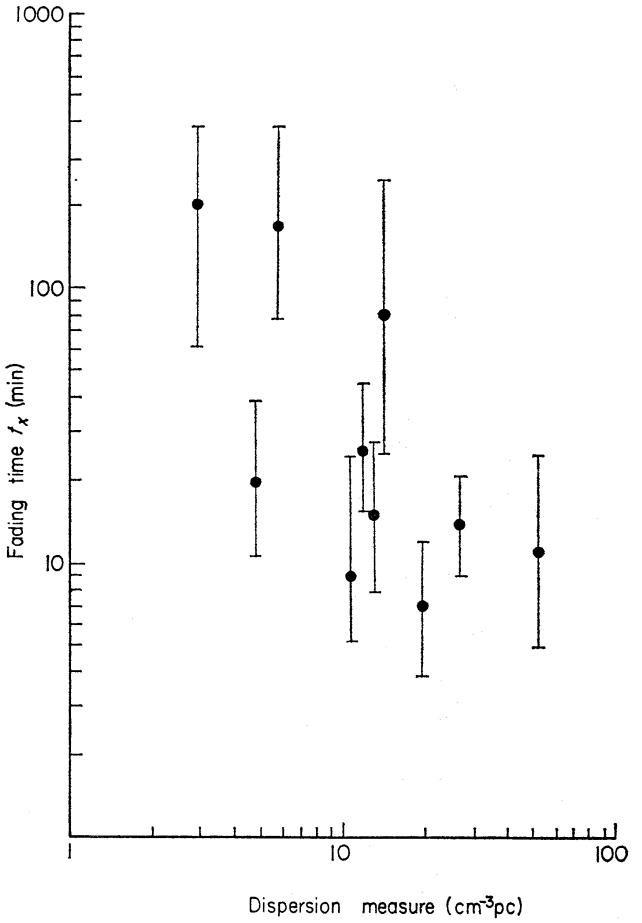

FIG. 9. *Logarithmic plot of mean time (t_x) between fading maxima at 408 MHz against dispersion measure for ten pulsars.*

have been observed but are not reliably established. The time scale, characterized by t_x, ranges from 7 minutes to 200 minutes among the ten sources at 408 MHz (Table I). No correlation has been found between t_x and pulsar period or duration. However, Fig. 9, showing a plot of t_x against dispersion measure, reveals a tendency for the lower dispersion pulsars to show slower variations.

The frequency width, characterized by B_h, similarly shows no correlation with intrinsic source parameters such as period or pulse length. Fig. 10, however, shows a correlation with dispersion measure; the higher dispersion pulsars show narrower frequency structure. The relationship is strong with a slope certainly steeper than -1; a line of slope -2 is drawn and is discussed in later sections. The points are well scattered even compared to the large errors; for example the four sources in the range 11·4–14·3 cm^{-3} pc show values of B_h differing by factors up to 26. Nevertheless, the conclusion from Fig. 10 is quite clear, that those electrons which are responsible for the dispersion are also responsible (perhaps indirectly) for the frequency structure.

The dependence of fading parameters on frequency has only been investigated for a few pulsars. No evidence has been found for a dependence of fluctuation index on frequency up to 922 MHz. The time scale t_x is longer at higher frequencies. Fig. 11 shows this for CP 1133 and CP 0328. If $t_x \propto f^n$, then n lies in the range $0{\cdot}3 \leqslant n \leqslant 1{\cdot}5$ for all the observations. For frequencies above 408 MHz $n \sim 0{\cdot}5$ appears to be typical.

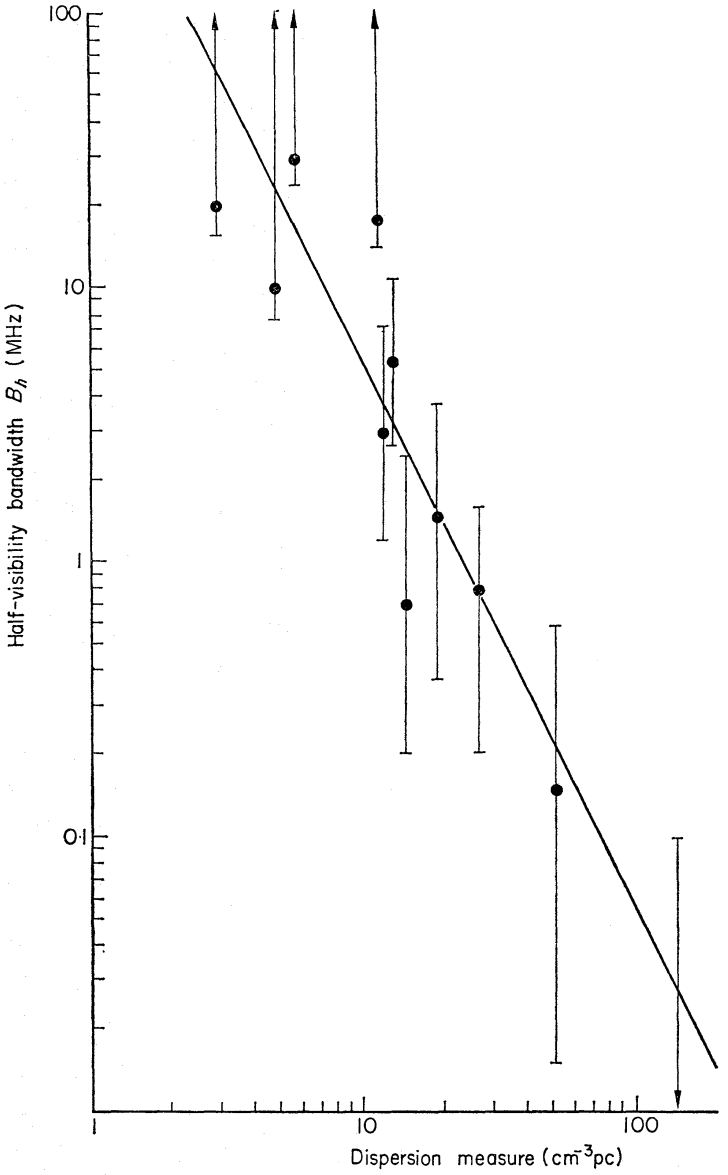

FIG. 10. *Logarithmic plot of half-visibility bandwidth (B_h) at 408 MHz against dispersion measure for eleven pulsars. A line of slope −2 is drawn.*

The variation of B_h with frequency has proved harder to determine. It is clear that narrower structure is obtained at lower frequencies. If $B_h \propto f^m$, then the values from Table II yield $m \sim 4$, $m \gtrsim 3{\cdot}2$ and $m \sim 5$ for CP 0328, CP 0808 and PSR 1749-28, respectively. The most precise result comes from the $1/e$ decorrelation widths of CP 0328 at 408 MHz and 610 MHz yielding $m \sim 3{\cdot}0$. The results of other observers (**19**), (**24**), (**25**), (**29**) when combined with the present results give m in the range 2–3. Taylor and Huguenin (private communication) have recently measured a decorrelation frequency width at several frequencies from 100 MHz to 400 MHz. They find that for eight pulsars m lies in the range 2·6 to 3·5 and they confirm the relationship with dispersion measure.

8. INTERSTELLAR SCINTILLATION AND PULSAR FADING

In the previous section evidence was given that the long term fading is definitely associated with the dispersing electrons. It now seems likely that most of the disper-

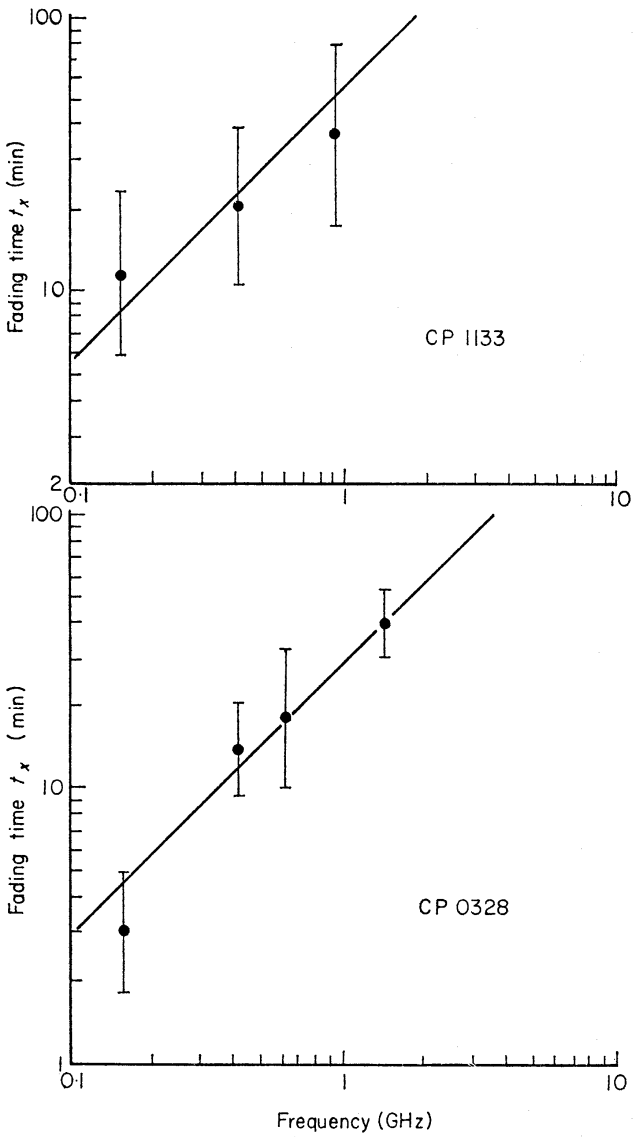

FIG. 11. *Logarithmic plot of time scale (t_x) against frequency for CP* 1133 *and CP* 0328. *Lines of slope* −1 *are drawn.*

sion is caused by a general interstellar electron distribution. The dispersion measures show a correlation with galactic latitude. In addition, uncomfortably low mean electron densities would be implied, if most of the dispersion was occurring in a dense electron cloud close to the source. We, therefore, assume that most pulsars lie within the galactic disc and that dispersion measures are (at least on average) a useful measure of distance. In estimating distances we will assume a uniform slab of 0·03 cm^{-3} electron density. Fig. 10 is thus taken as direct evidence that the frequency structure and fading is imposed on the pulses during their propagation through the interstellar medium.

A simple model of interstellar plasma irregularities is proposed. The irregularities in electron density are characterized by an r.m.s. deviation Δ cm^{-3} and a spatial a.c.f., which will be assumed to be a spherical gaussian of $1/e$ radius r_0 cm. The irregularities are assumed distributed uniformly (filling randomly a fraction α of the volume) in a galactic disc $\pm$ 200 pc in thickness.

The theory of scintillation in an extended medium is summarized in the next section and compared with the results in the following section.

9. THEORY OF SCINTILLATION IN AN EXTENDED MEDIUM

Some results of the theory of scattering in an extended medium are presented, derived chiefly from the work of Uscinski (**30**), (**31**).

A plane wave is assumed to be incident normally on a uniform scattering medium filling the half space $z \geqslant 0$. At a distance z into the medium, the wave may have suffered multiple scattering and the intensity remaining in the unscattered wave is reduced by a factor $\exp(-\beta z)$ on the incident wave. Here β is the coefficient of total scattering (**30**) and is given, for the scattering medium outlined in Section 8, by:

$$\beta = \pi^{1/2} b^2 \Delta^2 r_0 \lambda^2 \text{ cm}^{-1} \tag{2}$$

where λ cm is the wavelength and $b = 2{\cdot}82 \times 10^{-13}$ cm is the classical electron radius. In this and subsequent formulae a value of $\alpha = 1$ is assumed; other values are given by replacing Δ by $\alpha^{1/2}\Delta$. It should be noted that the quantity $(\beta z)^{1/2}$ bears a very close relationship to the r.m.s. phase deviation of the equivalent phase screen used by several authors (**14**), (**15**), (**25**).

A necessary consequence of traversing a distance z through the medium is that the plane wave is scattered into an angular spectrum with $1/e$ radius θ_s. In the extreme cases of weak and strong scattering approximate expressions exist:

$$\begin{aligned} \theta_s &= \theta_0 = \lambda/\pi r_0 \quad \text{for} \quad \beta z \ll 1 \\ \theta_s &= \theta_0 (\beta z)^{1/2} \quad \text{for} \quad \beta z \gg 1. \end{aligned} \tag{3}$$

In order to explain pulsar fading we require strong intensity fluctuations, the growth of which are controlled by two conditions. First we require strong scattering ($\beta z \geqslant 2$), and, second, we require that mutual interference between components of the scattered angular power spectrum must have occurred. Providing that the first condition holds, Uscinski (**31**) shows, in a note added in proof, that $A^2 \beta z \gg 6$ is a sufficient condition for this to occur (where $A = (\beta z_0)^{-1}$ and $z_0 = \pi r_0^2/2\lambda$, the Fresnel distance for the irregularities). If this inequality does not hold his analysis breaks down. Nevertheless intensity fluctuations may still develop for large z.

Consider the medium in two parts 0 to z_1 and z_1 to z. If large phase fluctuations have occurred at z_1 ($\beta z_1 \geqslant 2$) then, by analogy with a strong phase screen, intensity fluctuations will certainly have developed by a further distance $z_{\max} \sim z_0 (\beta z_1)^{-0{\cdot}6}$ (equation (27) of reference (**32**)). This would be true even if there was no scattering medium beyond z_1; the continued multiple scattering can only help to accelerate the production of intensity fluctuations. Following this argument further, it may be shown that the distance $z_1 + z_{\max}$ has a minimum value of $1{\cdot}3\, z_0 A^{0{\cdot}37}$. Therefore we can safely say that strong intensity fluctuations will have developed at total distances z exceeding this value. Thus the two conditions for strong intensity fluctuations may be stated:

$$\beta z \geqslant 2 \tag{4}$$

$$z \geqslant 1{\cdot}3 z_0 A^{0{\cdot}37}. \tag{5}$$

An independent approach comes from a ray path argument adopted by Scheuer (**14**), that rays passing through neighbouring irregularities in the equivalent screen cannot interfere unless $z\theta_s/2 \geqslant r_0$. It is interesting that this reduces to a condition very similar to (5).

If both inequalities (4) and (5) are obeyed, strong intensity fluctuations will be present and the lateral scale r_p of the pattern is given by the $1/e$ point of the spatial

a.c.f. (**31**). The two limiting cases are:

$$\begin{aligned} r_p &\sim 0{\cdot}8 r_0 \quad \text{for} \quad \beta z \ll 1 \\ r_p &\sim r_0 (2\beta z)^{-1/2} \quad \text{for} \quad \beta z \gg 1. \end{aligned} \tag{6}$$

For the intensity fluctuations to be visible in practice two further conditions must be obeyed. First the angular extent of the source must be small, for which an approximate condition is $z\psi < 1{\cdot}7 r_p$ (ψ is the half-power diameter of the source). The second condition is that the intensity pattern is not decorrelated across the receiver bandwidth. An approximate condition for this has been preliminarily obtained by Uscinski (**41**):

$$2\pi B \beta z^2 \theta_0{}^2 / c \leqslant 10. \tag{7}$$

An approximate but independent derivation of this condition is given in the Appendix.

The time scale of the scintillations is related to the lateral scale r_p via a velocity. For a rigid medium moving at a transverse velocity v the time scale is simply r_p/v. However, in a more realistic situation there will be random and systematic motions in the medium, which will imply that a single velocity is inadequate to relate the temporal and spatial variations.

10. COMPARISON OF RESULTS WITH THEORETICAL MODEL

The observations of conventional radio sources as well as those of pulsar intensity variations must be compatible with the proposed model of interstellar scintillation. An approach similar to that of Scheuer (**14**) will be used to investigate what constraints the observations impose on the parameters Δ and r_0, which describe the irregularities. The differences from Scheuer's analysis come in the somewhat more rigorous theory and in the new observations. The various constraints are as follows:

(i) Conventional small diameter sources do not vary on time scales of hours (or even days). It is proposed that this is due to angular diameter blurring of the scintillation pattern. The severest constraint comes from the observed steadiness of very small diameter sources at very high frequencies where the lack of scintillation cannot be due to bandwidth smoothing. The quasar 3C 454·3 has been observed to have over 80 per cent of its flux at 6-cm wavelength from a diameter less than 6×10^{-4} sec arc (**33**). Using equation (6) and a distance of 300 pc through the medium, the condition for angular diameter blurring leads to:

$$\Delta r_0{}^{-1/2} > 6{\cdot}5 \times 10^{-12} \text{ cm}^{-3{\cdot}5}. \tag{8}$$

(ii) If inequality (7) does not hold in an angular diameter measurement of a radio source, amplitude scintillation will not be observed but the apparent diameter will be increased to a lower limit of θ_s given by equation (3). Observations of very small diameters at very low frequencies, therefore, allow us to put an upper limit on θ_s. The strictest limit (Scheuer (**14**)) comes from the observation of a component of the Crab nebula with a diameter $\leqslant 0{\cdot}3$ sec arc at 38 MHz (**34**). Assuming a distance of 2 kpc (**8**), this leads to:

$$\Delta r_0{}^{-1/2} \leqslant 2{\cdot}7 \times 10^{-10} \text{ cm}^{-3{\cdot}5}. \tag{9}$$

(iii) The pulsars show strong intensity fluctuations; the two inequalities (4) and (5) must therefore be obeyed. The strictest limits come from the observations of nearby pulsars at the higher frequencies. Deep fading has been observed at 922 MHz

from CP 1133, for which a distance of 150 pc is estimated (Section 8). Conditions (4) and (5) lead to:

$$\Delta r_0^{1/2} \gtrsim 5{\cdot}4 \text{ cm}^{-2{\cdot}5} \tag{10}$$

$$\Delta r_0^{1.16} \gtrsim 2{\cdot}2 \times 10^{-18} \text{ cm}^{-4{\cdot}16}. \tag{11}$$

(iv) We now compare the results for the pulsar frequency structure with the theory. If inequality (7) is replaced by an equality it gives a theoretical expression for B_h, the quantity measured in the bandwidth experiment. This can be re-expressed using equations (2) and (3) as:

$$B_h \simeq \frac{8{\cdot}9c}{\Delta^2 r_0^{-1} b^2 z^2 \lambda^4} \text{ Hz}. \tag{12}$$

The importance of this relation is the variation of $B_h \propto z^{-2}\lambda^{-4}$. As discussed in Section 8, the dispersion measure of each pulsar is on average proportional to its distance through the scattering medium. Hence a slope of -2 is predicted in Fig. 10. The observed points are in reasonable agreement with such a line and thus the model satisfactorily explains the results. The observed dependence of B_h on frequency is closer to the third power than the fourth as predicted. However, the steepness of the observed dependence on frequency will be accepted, at this stage, as evidence that the scintillation model is correct in principle. In order to put the frequency structure measurements quantitatively into the model, the results of Fig. 10 will be represented by a single pulsar. We take the following values for CP 0328:

$$z = 0{\cdot}8 \text{ kpc}$$

$$B_h = 0{\cdot}8 \text{ MHz at } \lambda = 73{\cdot}5 \text{ cm}.$$

Substituting into equation (12) this leads to:

$$\Delta r_0^{-1/2} \sim 1{\cdot}5 \times 10^{-10} \text{ cm}^{-3{\cdot}5} \tag{13}$$

(v) Finally we compare the time scale data with the model. An effective scale size for the intensity pattern is obtained by combining equations (6), (2) and (12):

$$r_p \simeq 5{\cdot}8 \times 10^7 (B_h \text{ MHz})^{1/2} (z \text{ kpc})^{1/2} \lambda \text{ cm}.$$

If this is now combined with the time scale t_x we can define an effective velocity $v_{\text{eff}} = 2{\cdot}6 r_p / t_x$, leading to:

$$v_{\text{eff}} \simeq 24 (z \text{ kpc})^{1/2} (B_h \text{ MHz})^{1/2} \lambda (t_x \text{ min})^{-1} \text{ km s}^{-1}.$$

v_{eff} has been evaluated from the observed B_h and t_x for each pulsar at 408 MHz. The values lie in the range 12 to 250 km s^{-1} (except for PSR 2045-16, giving $\geqslant 580$ km s^{-1}). Velocities of about 50 km s^{-1} are expected from the Earth's motion and differential galactic rotation and are of similar magnitude to v_{eff} except in a few cases. The results of Section 7 show that the time scale is approximately proportional to frequency as predicted by the theory.

II. DISCUSSION OF THE MODEL

Fig. 12 is a logarithmic plot of the Δ, r_0 plane, as first plotted by Scheuer (**14**). The constraints obtained in the previous section are plotted as lines. We are trying to locate a single point, representing the interstellar irregularities. Such a point must

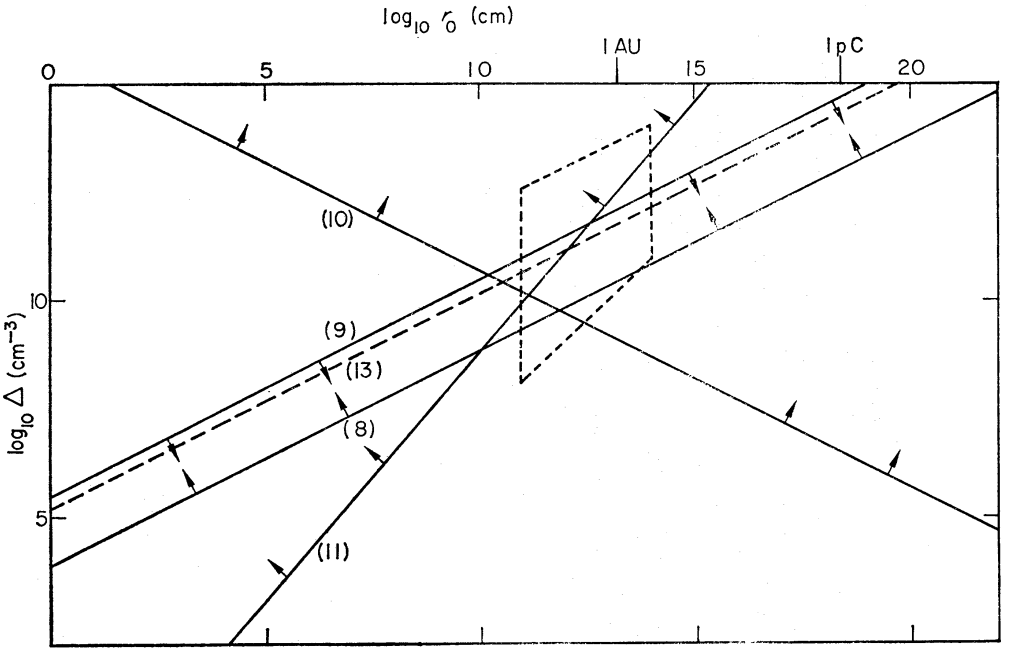

FIG. 12. *Parameters of the interstellar plasma irregularities* Δ, r_0 *on logarithmic scales. The various limiting lines discussed in the text are shown with their equation numbers indicated. The area outlined by a dashed line is that considered by Salpeter* (**15**).

lie beyond each solid line in the direction of the arrows and close to the dashed line representing the result of the bandwidth experiment (equation (13)). It is seen that there is a small allowed region approximately centred on:

$$\Delta = 4{\cdot}7 \times 10^{-5}\ \mathrm{cm}^{-3}$$
$$r_0 = 10^{11}\ \mathrm{cm}. \qquad (14)$$

The ranges allowed are factors of about 2 and 4 in either direction on Δ and r_0 respectively.

The fact that a single point *can* be reconciled with all the observations is regarded as a success for the model. However, this does not prove that the irregularities *are* well-defined regions of a unique scale r_0 and density deviation Δ, nor does it prove that they are uniformly distributed in the galactic disc. Nevertheless we pursue the specific model further (as it is compatible with the observations) and re-examine the applicability of the theory and the predictions from it.

Using the values of equation (14), we obtain at a frequency f MHz:

$$\beta = 0{\cdot}52\ (408/f)^2\ \mathrm{pc}^{-1}$$
$$A = 0{\cdot}027\ (f/408)$$
$$z_0 = 71\ (f/408)\ \mathrm{pc}. \qquad (15)$$

The analysis of Uscinski (**30**), (**31**) is strictly applicable only if $A^2\beta z \gg 6$, which becomes, independently of frequency:

$$z \gg 62\ \mathrm{kpc}. \qquad (16)$$

The pulsars observed are thought to lie within about 2 kpc and thus inequality (16) does not hold. The medium is therefore behaving like an extended phase screen and the scattered waves will not be randomly phased (**35**). This might produce fluctua-

tion indices exceeding one and intensity distributions differing from the limiting exponential form. It may be significant that the low dispersion pulsars have given fluctuation indices exceeding unity at 408 MHz (e.g. CP 1133). Another consequence of (16) is that the derivation of equation (12) for B_h may no longer be valid. We suggest that this might account for the observed dependence of B_h on frequency as the third power instead of the predicted fourth.

A further approximation in the analysis is that the pulsars have been represented by sources of plane waves incident on the scattering medium. In practice they are probably extended objects embedded in the medium. No proper analysis exists for this situation, but the theory will probably be satisfactory providing that the transverse linear dimension of the emitting region is smaller than the scale of the pattern r_p. This requires emitting regions smaller than about 10^4 km.

The values of v_{eff} derived from the time scale observations show no detailed correlation with transverse velocities computed from the Earth's motion and differential galactic rotation for each measurement. We conclude that shearing or random motions with velocities up to 100 km s^{-1} are typical for the irregularities.

Scheuer (**14**), in considering the role of interstellar scintillation in explaining the pulsar intensity variations, found some difficulties with the observations then available. These problems have largely been overcome by a better understanding of the frequency structure, and by the separation of the slower variations from CP 1919 into two regimes. The relatively wide band one minute bursts from this source are distinct from the interstellar scintillations, but could still be caused by a diffraction 'screen' close to the source (as suggested by Scheuer).

Salpeter (**15**) tackled the problem differently and proposed a range of values of Δ and r_0. He postulated a range r_0 from 10^{11} cm to 10^{14} cm, each with its own (functionally related) Δ. His model would be a line with a slope γ lying in the dashed area on Fig. 12 rather than a point. The conditions for scintillation are picked out by the application of the focusing condition from the equivalent phase screen at the frequency of observation. Salpeter's approximate analysis predicts the dependence of frequency structure width and time scale on frequency and distance. Using his expressions the present observations imply that his exponent $\gamma \lesssim 0$, which is just compatible with his postulated $0 < \gamma < 0{\cdot}5$. He also suggests that the frequency a.c.f. of the fluctuations might show two widths; the result, however, for CP 0328 at 408 MHz (Fig. 7) shows a smooth curve over the range 60 KHz to 2·5 MHz. It is felt that a more exact theory is necessary for detailed comparison with the observations. Analysis is needed, as discussed in Section 14, of 'focusing' conditions in extended media, allowing also non-gaussian spatial power spectra for the density deviations.

12. IRREGULARITIES IN THE INTERSTELLAR PLASMA

The proposed scale of the irregularities is very small (1·6 $R_\odot$) on a galactic scale. The possibility that these are actual stellar coronae has been examined, but number densities for stars are too small. The condition for an effective scattering medium is that there must be a very large number of irregularities in a column of length say 100 pc with the diameter of a Fresnel zone at 408 MHz; this leads to a minimum number density for the irregularities of 2×10^{12} pc^{-3}. In the expressions given up to this point the irregularities are assumed to fill the available volume. However, if only a fraction α of the volume is (randomly) filled, the r.m.s. density Δ must be replaced by $\alpha^{1/2}\Delta_\alpha$ in all formulae. Knowing the volume of each irregularity the

minimum number density implies that $\alpha \gg 5 \times 10^{-10}$ and thus $\Delta_\alpha \ll 2$ cm^{-3}. The mean electron density contributed by the irregularities is $\alpha\Delta_\alpha$ which is a maximum of $4{\cdot}7 \times 10^{-5}$ cm^{-3} as $\alpha \leqslant 1$. Thus we are concerned with a maximum of about 0·15 per cent of the total number of electrons (taking a mean density of 0·03 cm^{-3}).

Recently several authors (**36**), (**37**), (**38**) have discussed the contributions to pulsar dispersions from the cool interstellar clouds and the hot intercloud medium. Hjellming *et al.* (**37**) show that the intercloud medium is largely responsible for the pulsar dispersions. It follows that the plasma irregularities causing the scintillation are probably situated in the intercloud medium. For thermal electrons in 10^{-6} gauss in this region the gyro-radius will be about 10^6 cm, which is much smaller than the irregularities. It therefore seems likely that the irregularities will be linked to a microstructure in the magnetic field. Disturbances such as Alfvén waves suggest themselves; in the intercloud medium Alfvén velocities are typically 10–100 km s^{-1}, compatible with those deduced from the observations.

A possible excitation mechanism for such waves has been suggested by Wentzel (**39**). He shows that if cosmic rays are caused to stream along magnetic field lines (e.g. in regions of compression between H I clouds), they will excite hydromagnetic waves with a wavelength equal to their gyro-radius. Thus in a one microgauss field, electrons of 5 MeV or protons of 0·01 MeV, will excite wavelengths of 10^{11} cm. Some longitudinal component of the waves must be present to allow density changes. The circumstances giving rise to such waves must be widespread in order to explain the strong correlation with dispersion measure shown in Fig. 10. No further consideration will be given here of the possible origins and stability of interstellar plasma irregularities; we have been chiefly concerned with presenting observational evidence for their existence.

13. PREDICTIONS FROM THE MODEL

Having analysed the pulsar fading results in the light of a simple model of interstellar scintillation, we will now summarize the predictions from the model.

The conditions for the observation of scintillation are first given for a source seen through z kpc of medium at a frequency f MHz.

(i) Strong scattering condition: $f \lesssim 6600\ (z \text{ kpc})^{1/2}$ MHz.
(ii) Interference condition: $f \lesssim 6150\ (z \text{ kpc})^{0.73}$ MHz.
(iii) Receiver bandwidth B: $B \lesssim 0{\cdot}61\ (z \text{ kpc})^{-2}\ (f/408)^4$ MHz.
(iv) Source half-power diameter: $\psi \lesssim 3{\cdot}8 \times 10^{-7}\ (z \text{ kpc})^{-3/2}\ (f/408)$ sec arc.

Pulsars are the only objects known to satisfy all these conditions; other sources do not satisfy condition (iv). Interstellar scattering will occur for any observation in which condition (i) is satisfied. The radiation is scattered into a cone of angular half-width θ_s

$$\theta_s \sim 10^{-3}(408/f)^2(z \text{ kpc})^{1/2} \text{ sec arc.}$$

Measurements of angular diameters are therefore subject to a minimum observable diameter of θ_s provided that one of the conditions (iii) or (iv) does not hold or integration is taken over many intervals of the fading time. This may be tested by observation of radio sources at low frequencies. If small enough (intrinsic) diameter extra-galactic sources could be measured, a dependence of apparent diameter on galactic latitude should be found. Measurements of angular diameters at say 38 MHz using interplanetary scintillation might be the most sensitive test of this.

14. CONCLUSION

Further experiments on pulsar intensity variations can now be suggested. More work is needed on many sources to compare the short term fluctuations with those of CP 0328 and CP 1919, which show time scales of seconds and minutes respectively. It would be useful to establish whether there is a range of behaviour between these extremes or perhaps two well-defined classes of pulsar. Does the duration of the short term variability correlate with other source parameters? The contrast between the erratic pulses reported from NP 0531 and the steady pulses from PSR 0833-45 is surprising from two pulsars showing several common features. The variations over days to months require further investigation. In particular the frequency range over which these changes occur has not yet been established.

Experiments to investigate further the interstellar fading component include spectral observations of a larger sample of sources, monitoring the time scale of the variations (an annual change might be found due to the changing direction of the Earth's velocity), spaced receiver observations to detect the motion and possibly measure the scale of the intensity pattern, and high frequency measurements to find at what frequency the strong scattering condition breaks down.

The analysis in the theoretical model has several short comings, suggesting some further lines of theoretical work.

(i) The analysis of a linearly extended source embedded in the scattering medium requires detailed analysis.

(ii) Motion of the extended medium, including shearing, is inadequately related to the observable temporal variations.

(iii) The irregularities may be better described by a spatial power spectrum which is flatter than the assumed gaussian.

(iv) The model leads to a medium which is behaving like an extended phase screen. There is inadequate analysis of the fluctuation parameters (including spectral width) for waves scattered by such a medium, where intensity variations have just barely developed.

To conclude, we note that the pulsar intensity variations have been shown to contain at least two categories. A pulse-to-pulse variation occurs at the source, simultaneously over a wide frequency range. In contrast a narrow band slow fading is imposed during the propagation of the waves through the interstellar medium. The steep dependence of the frequency structure width on dispersion measure and frequency is strong evidence in favour of an interstellar scintillation process. A model, assuming well-defined irregularities of a unique size and strength, fits the results well; the deduced values are an r.m.s. electron density deviation $4{\cdot}7 \times 10^{-5}$ cm^{-3} and size 10^{11} cm. This deduction comes from the limits imposed by several observations, interpreted by the model. If a flatter than assumed spatial spectrum is present, the values may deviate by perhaps an order of magnitude. It seems, however, that a weak widespread distribution of very small scale irregularities must be responsible for the fading and frequency structure observed in pulsar intensities.

ACKNOWLEDGMENTS

I thank Sir Bernard Lovell for making available the facilities at Jodrell Bank. I thank Dr A. G. Lyne and Dr G. de Jager for help with the observations. I thank Professor J. G. Davies for help with the computing. I thank Professor F. G. Smith

for helpful discussion and Dr B. J. Uscinski for valuable discussions on scattering in an extended medium and for making available some preliminary results prior to publication.

University of Manchester, Nuffield Radio Astronomy Laboratories, Jodrell Bank, Cheshire.

Present address: *Department of Applied Physics and Information Science, University of California at San Diego, La Jolla, California 92037, U.S.A.*

Received in original form 1969 *November* 24.

REFERENCES

(1) Hewish, A., Bell, S. J., Pilkington, J. D. H., Scott, P. F. & Collins, R. A., 1968. *Nature, Lond.*, **217,** 709.
(2) Davies, J. G., Horton, P. W., Lyne, A. G., Rickett, B. J. & Smith, F. G., 1968. *Nature, Lond.*, **217,** 910.
(3) Drake, F. D., Gundermann, E. J., Jauncey, D. L., Comella, J. M., Zeissig, G. A. & Craft, H. D., 1968. *Science*, **160,** 503.
(4) Tanenbaum, B. S., Zeissig, G. A. & Drake, F. D., 1968. *Science*, **160,** 760.
(5) Guélin, M., Guilbert, J., Huchtmeier, W. & Weliachew, L., 1968. *Nature, Lond.*, **221,** 249.
(6) Gordon, C. P., Gordon, K. J. & Shalloway, A. M., 1969. *Nature, Lond.*, **222,** 129.
(7) de Jager, G., Lyne, A. G. & Pointon, L., 1969. Private communication.
(8) Trimble, V. L., 1968. *Astr. J.*, **73,** 535.
(9) Smith, F. G., 1968. *Nature, Lond.*, **218,** 325.
(10) Smith, F. G., 1968. *Nature, Lond.*, **220,** 691.
(11) Staelin, D. H. & Reifenstein, E. C., 1969. *Astrophys. J.*, **156,** L121.
(12) Radhakrishnan, V., Cooke, D. J., Komesaroff, M. M. & Morris, D., 1969. *Nature, Lond.*, **218,** 443.
(13) Ekers, R. D., Lequeux, J., Moffet, A. T. & Seielstad, G. A., 1969. *Astrophys. J.*, **156,** L21.
(14) Scheuer, P. A. G., 1968. *Nature, Lond.*, **218,** 920.
(15) Salpeter, E. E., 1969. *Nature, Lond.*, **221,** 31.
(16) Lyne, A. G. & Rickett, B. J., 1968. *Nature, Lond.*, **218,** 326.
(17) Lyne, A. G. & Rickett, B. J., 1968. *Nature, Lond.*, **219,** 1339.
(18) Rickett, B. J., 1969. *Nature, Lond.*, **221,** 158.
(19) Scott, P. F. & Collins, R. A., 1968. *Nature, Lond.*, **218,** 230.
(20) Davies, R. D., Ponsonby, J. E. B., Pointon, L. & de Jager, G., 1969. *Nature, Lond.*, **222,** 933.
(21) Staelin, D. H. & Reifenstein, E. C., 1969. *Science*, **162,** 1481.
(22) Comella, J. M., Craft, H. D., Lovelace, R. V. E., Sutton, J. M. & Tyler, G. L., 1969. *Nature, Lond.*, **221,** 454.
(23) Robinson, B. J., Wielebinski, R., Cooper, B. T. C., Gardner, F. F. & Landecker, T. L., 1969. *Nature, Lond.*, **218,** 1143.
(24) Komesaroff, M. M., McCulloch, P. M., Hamilton, P. A. & Cooke, D. J., 1968. *Nature, Lond.*, **220,** 360.
(25) Lovelace, R. V. E. & Craft, H. D., 1968. *Nature, Lond.*, **220,** 875.
(26) Slee, O. B., Komesaroff, M. M. & McCulloch, P. M., 1968. *Nature, Lond.*, **219,** 342.
(27) Conklin, E. K., Howard, H. E., Craft, H. D. & Comella, J. M., 1968. *Nature, Lond.*, **219,** 1238.
(28) Drake, F. D. & Craft, H. D., 1968. *Nature, Lond.*, **220,** 231.
(29) Huguenin, G. R. & Taylor, J. H., 1969. *Astrophys. J. Lett.*, **3,** 107.
(30) Uscinski, B. J., 1968. *Phil. Trans. R. Soc.*, **A262,** 609.
(31) Uscinski, B. J., 1968. *Proc. R. Soc.*, **A307,** 471.
(32) Bramley, E. N. & Young, M., 1967. *Proc. I.E.E., III*, **97,** 11.
(33) Kellerman, K. I., Clark, B. G., Bare, C. C., Rydbeck, O., Ellder, J., Hansson, B., Kollberg, E., Hoglund, B., Cohen, M. H. & Jauncey, D. L., 1968. *Astrophys. J.*, **153,** L209.
(34) Bell, S. J. & Hewish, A., 1967. *Nature, Lond.*, **213,** 1214.

(35) Ratcliffe, J. A., 1956. *Rep. Prog. Phys.*, **19**, 188.
(36) Prentice, A. J. R. & Ter Haar, D., 1969. *Nature, Lond.*, **222**, 964.
(37) Hjellming, R. M., Gordon, C. P. & Gordon, K. J., 1969. *Astr. Astrophys.*, **2**, 202.
(38) Davies, R. D., 1969. *Nature, Lond.*, **223**, 355.
(39) Wentzel, D. G., 1969. *Astrophys. J.*, **156**, L91.
(40) Little, L. T., 1968. *Plan. Space Sci.*, **16**, 749.
(41) Uscinski, B. J., 1969. Private communication of preliminary results.

APPENDIX

FREQUENCY WIDTH OF STRONG SCINTILLATION IN AN EXTENDED MEDIUM

Little (**40**) has analysed the reduction in scintillation index from a localized diffracting screen at a distance z, caused by observing with a non-zero receiver bandwidth. His results show that the scintillation visibility is a function of the parameter $D = \pi z\theta_s^2\Delta_\nu/c$. Here Δ_ν is the $1/e$ halfwidth of the gaussian assumed bandpass, and θ_s is the halfwidth of the scattered angular power spectrum. Replacing Δ_ν by $B/1{\cdot}65$ for a rectangular bandwidth B and using Little's result that the visibility falls to one-half at $D = 4$, we obtain the half-visibility bandwidth:

$$B_h \simeq 6{\cdot}6c/\pi z\theta_s^2. \tag{17}$$

This is explained in a simplified way by the following argument (first put forward by Hewish).

The details of the diffraction pattern at a given frequency are determined by the path differences between various components of the scattered angular spectrum. These path differences are typically $z\theta_s^2/2$ for a scattering angle θ_s. Some smearing of the scintillation patterns across a bandwidth B will occur if the coherence length c/B is less than this. The condition for reduction of scintillation thus, $z\theta_s^2/2 \gtrsim c/B$.

In an extended medium similar arguments apply, but the chief difference is that the scattering angle is now a function of distance. We, therefore, consider an effective path length difference as $\frac{1}{2}\int_0^z \theta_s^2 dz$. Assuming that the two equations (3) apply exactly for distances $\lesseqgtr 2\beta^{-1}$ the integral becomes:

$$\begin{aligned}\tfrac{1}{2}\int_0^z \theta_s^2 dz &= \tfrac{1}{2}\int_0^{2\beta^{-1}} \theta_0^2 dz + \tfrac{1}{2}\int_{2\beta^{-1}}^z \theta_0^2 \beta z dz \\ &= \beta\theta_0^2 z^2/4.\end{aligned}$$

If this effective path length is substituted for $z\theta_s^2/2$ in equation (17) we obtain:

$$B_h \sim \frac{23c}{\Delta^2 r_0^{-1} b^2 z^2 \lambda^4}. \tag{18}$$

Where expressions for β and θ_0 have been introduced from equations (2) and (3).

Uscinski (**41**) has derived a result which reduces to equation (12). The functional agreement with (18) is exact; the results differ by a constant factor of 2·6. Uscinski's result is used as it is based on more exact arguments than those presented above.